Supporting Information

Schmaier et al. 10.1073/pnas.0906436106

SI Materials and Methods

Animals. GPVI-deficient and Lyn-deficient mice have been previously described (1, 2). Wild-type C57/BL6 mice were purchased from Charles River Laboratories. All of the mice used for study were maintained in the animal facility of the University of Pennsylvania in accordance with National Institute of Health guidelines and approved animal protocols.

Antibodies and Reagents. Anti-human GPVI monoclonal antibodies HY101 and 6B12 were produced as previously described (3) and were conjugated with Alexa Fluor-647 using the Monoclonal Antibody Labeling Kit purchased from Molecular Probes. Convulxin, AYPGKF peptide, and PE-conjugated anti-murine CD62P (P-selectin) antibody were purchased from previously described sources (4). CRP was obtained from R. Farndale (Cambridge, U.K.). FITC-conjugated polyclonal anti-rabbit Ig was purchased from BD PharMingen. JON/A, JAQ1, and Leo.H4 monoclonal antibodies were purchased from Emfret Analytics. Type-I fibrillar collagen (1 mg/ml) derived from equine tendon was purchased from Chronolog. Purified acid-soluble fibrillar collagen (PureCol) derived from bovine hide (3 mg/ml) was purchased from Inamed. Rat anti-mouse CD41 (integrin $\alpha 2_b$) monoclonal antibody was purchased from BD Biosciences. Alexa-Fluor 488 and 647 Monoclonal Antibody Labeling Kits, Alexa-Fluor 647-conjugated human fibrinogen, and Alexa-Fluor 594-conjugated phalloidin were purchased from Invitrogen. Murine stem cell factor, IL-3, and IL-6 were purchased from PeproTech. Anti-GFP, anti-Lyn, anti-Fyn, anti-Syk, and anti-Btk rabbit polyclonal antibodies were obtained from Santa Cruz Biotechnology. Anti-FcRγ chain rabbit polyclonal antibody was obtained from Abcam. Antiphosphotyrosine mouse monoclonal antibody 4G10 was obtained from Millipore. Anti-phospho Src family (Y416), anti-phospho Lyn (Y507), and anti-phospho Syk (Y525/526) rabbit polyclonal antibodies, and anti-Src rabbit monoclonal antibodies were obtained from Cell Signaling.

Retrovirus Production. The cDNA of human GPVI was subcloned into the *p*-GEM-T Easy vector (Promega), and site-directed mutagenesis to remove the PRD was performed using the Stratagene QuikChange site-directed mutagenesis kit. The oligonucleotide used for site-directed mutagenesis has been previously described (5). Wild-type and PRD deleted GPVI were subcloned into XhoI/HpaI sites of the murine stem cell virus MigR1 vector with an IRES-GFP inserted before the polyadenylation signal, as described previously (6). Production and titering of retrovirus was performed as previously described (7). For RBL-2H3 cell infections, wild-type GPVI and GPVI lacking the proline-rich domain were subcloned into XbaI/EcoRI sites of the HFUW lentiviral vector (kind gift from E. Brown, Department of Cancer Biology, University of Pennsylvania School of Medicine). The lentiviral vectors were packaged using HEK 293T cells.

Fetal Liver Cell Reconstitution. Reconstitution of lethally irradiated animals with stem cells derived from fetal liver was performed as previously described (6). Briefly, fetal liver cells from *gp6*$^{-/-}$ embryos at E14 to E16 were harvested, and mononuclear cells were isolated using Lympholyte (Cedarlane Labs) gradient and cultured overnight in IMDM with 10% FBS in the presence of 100 ng/ml murine stem cell factor, 20 ng/ml IL-3, and 10 ng/ml IL-6. The cells were then spin-infected twice with *gp6* retroviruses at a multiplicity of infection equal to 5 virions per cell. A total of 1×10^6 cells (250 μl per mouse) were retro-orbitally injected into 8- to 10-week-old C57/BL6 donor mice that received a lethal dose of 900 cGy total body irradiation. All platelet studies were performed at least 6 weeks after transplantation.

GPVI Antibody Staining. For mice, a drop of blood was collected from the tail vein, whereas for humans a drop of blood was obtained from a finger-stick into 100 μl of Tyrode's buffer (137 mM NaCl, 1 mM $MgCl_2$, 2.7 mM KCl, 3.3 mM NaH_2PO_4, 1 g/L BSA, 5.6 mM glucose, 20 mM Hepes, pH 7.4) containing 15 U/ml heparin. Diluted whole blood was incubated with Alexa-Fluor 647-conjugated HY101 anti human GPVI antibody at 2 μl/ml for 30 min at room temperature, and samples were analyzed using flow cytometry.

Murine Blood Collection. Mice were anesthetized with 16 μg/g body-weight tribromoethanol, and 100 μl of whole blood was collected by retro-orbital bleeding with a heparinized capillary tube. Platelet-rich plasma (PRP) was obtained by diluting whole blood 1:2 in Tyrode's buffer and performing centrifugation at $100 \times g$ for 4 min.

Platelet Spreading Assay. Lab-Tek II chamber slides (Thermo Fischer Scientific) were coated with type-I fibrillar collagen at 30 μg/ml in 50-μM acetic acid for 16 h at 4 °C, washed three times with PBS, and blocked with BSA 1 mg/ml in PBS for 30 min at room temperature. PRP was diluted to 2×10^7 platelets per milliliter in modified Tyrode's buffer (137 mM NaCl, 20 mM Hepes, 2.7 mM KCL, 3.3 mM NaH_2PO_4, 5.6 mM glucose, 1 g/L BSA, pH 7.4) containing 1 mM $MgCl_2$, and 5×10^6 platelets were incubated on the collagen-coated chambers for 45 min at 37 °C. Fixation, permeablizing, and staining were performed as previously reported (8). Following three washes in PBS, adherent platelets were fixed with 3% PFA in PBS for 40 min, washed three times in PBS, and permeablilized with 0.3% Triton X-100 in PBS with BSA 1 mg/ml for 2 h. After three washes in PBS, platelets were incubated with anti-GFP rabbit polyclonal antibody (10 μl/ml) for 16 h at 4 °C, washed three times in PBS, and incubated with FITC-conjugated polyclonal anti-rabbit Ig (2 μl/ml) for 2 h at room temperature. Filamentous actin was stained with Alexa-Fluor 594-conjugated phalloidin (25 μl/ml) for 45 min at room temperature. Platelet spreading was imaged as previously described (6), and only platelets with both GFP and actin staining were visualized. Platelet surface area was measured in pixels using Image J software (National Institutes of Health) particle analysis. Particles of sizes from 250 to 4,050 pixels, which represented those well-separated platelets, were measured.

Platelet Stimulation Assays. PRP was diluted to 2.5×10^7 platelets per milliliter in modified Tyrode's buffer, and 2.5×10^6 platelets were stimulated with varying concentrations of convulxin for 10 min at 37 °C in the presence of PE-conjugated anti-murine P-selectin antibody (2 μl/ml) and 1 mM $CaCl_2$ and $MgCl_2$. In time-course assays, 2.5×10^6 platelets were stimulated for the time indicated in the presence of 100 μg/mg Alexa-Fluor 647-conjugated fibrinogen, and the reaction was stopped by addition of 1% PFA for 5 min followed by washing. In time-course assays using JON/A antibody binding, platelets were stimulated with 10-nM convulxin for the time indicated at room temperature, and the reaction was stopped by addition of 1% PFA for 5 min

followed by washing. Platelets were then stained by addition of PE-conjugated JON/A antibody (10 μl/ml) for 30 min at room temperature. Fibrinogen and antibody binding were measured with a FACSort (BD Biosciences), and the data were analyzed with FlowJo 6.3.1 software (Tree Star).

Ca^{2+} Mobilization Assays. RBL-2H3 cells were labeled with Fura-2 a.m. (Molecular Probes), and calcium signaling was detected as previously described (3).

Fabrication of Microfluidic Devices, Collagen Patterning, and Whole-Blood Flow Assay. Fabrication of microfluidic devices and microfluidic collagen patterning was performed as previously described (9). Channels were initially filled with 1 mg/ml BSA in HBS to ensure that no bubbles were trapped in the channel. Whole blood from reconstituted mice was collected retro-orbitally as described above. Blood was incubated with JAQ-1 antibody at 25 μg/ml for 10 min, to block any wild-type mouse GPVI on platelets derived from host precursors that escaped bone marrow ablation, and with 5 μg/ml Leo.H4 monoclonal antibody, to prevent aggregate formation for ease of analysis. Whole blood from $lyn^{-/-}$ or $fyn^{-/-}$ mice and wild-type controls was collected in 93 μM PPACK (Hematologic Technologies, Inc.), labeled with Alexa-Fluor 488-conjugated CD41 antibody, and incubated with 5 μg/ml Leo.H4. A volume of 70 μl of whole blood was placed on the inlet of the device and withdrawn by a syringe pump (Harvard Apparatus PHD 2000) for up to 4 min at flow rates of 5 μl/min to achieve a full channel width-averaged wall shear rate of $\bar{\gamma}_{chan} = 1{,}000\ s^{-1}$.

Image Capture and Analysis. The adhesion of GFP+ platelets or fluorescently labeled platelets was monitored continuously by epifluorescence microscopy. For blood from reconstituted animals, images were captured continuously with a 60- to 200-ms exposure time depending on the percentage of GFP+ platelets in each mouse at an interval of 100 ms using Slidebook software (Intelligent Imaging Innovations). Every new rolling platelet that appeared was tracked in subsequent frames to determine if it ultimately adhered firmly to the collagen surface or if it continued to roll but did not adhere. All analyses were performed with the observer blinded to the identity of the sample. All image stacks were analyzed frame-by-frame in Slidebook. Any platelet that was captured by fluorescent imaging was presumed to be rolling along the collagen surface, as nonrolling GFP+ platelets, leukocytes, and red blood cells moved too fast to be visualized. Each frame was analyzed to determine if a new platelet began to roll on the patterned collagen surface. Firmly adherent platelets were defined as ones that did not change position for at least 30 frames. Platelets that came in contact with the wall of the flow chamber were not counted. Platelets that rolled as a preformed clump or adhered to preexisting platelet clumps and not to the collagen surface directly were not counted. Each experiment was only analyzed as long as individual platelet-collagen interactions could be distinguished. In determining the number of frames each adherent platelet spent rolling, the last frame before the platelet changed position for a final time was counted. Thus, a platelet that was permanently adhered by the first frame in which it was observed was counted as rolling for zero frames, and the rolling time consisted only of the interval before the frame in which the platelet appeared. The adhesive efficiency for each image stack was determined by calculating $a/(a + r)$, where a equals the number of platelets that permanently adhere and r equals the number of platelets that roll along collagen but do not adhere. The time each adherent platelet spent in the rolling phase was calculated as $(F)(Ex) + (F + 1)(Int)$, where F equals the number of frames the platelet spent rolling, Ex equals the exposure time per frame, and Int equals the interval time between captures, which was 100 ms for all experiments. Images were captured using a CCD camera (C9300–201 Hamamatsu) mounted on an inverted microscope (Nikon Eclipse TE2000-U) with a 300 W Xenon lamp (Perkin–Elmer Optoelectronics) through a Lambda DG-4 high-speed filter changer (Sutter Instruments) used at 470 nm Ex/525 nm Em. For blood flow experiments from $Lyn^{-/-}$ or $Fyn^{-/-}$ mice or wild-type controls, the collagen patch was defined using Image J software (National Institutes of Health). The average background of the upstream region was calculated for each column and those values were subtracted from the reaction zone pixel values to correct for background gradients across the width of the channel. Surface coverage was calculated by dividing the area of pixels with a value greater than zero by the area of the collagen patch.

Production of GST-Fusion Proteins and Expression of Recombinant SFKs and Nef. GST fusion proteins of the GPVI C-tail were prepared from cDNA encoding the WT or PD GPVI sequence beginning from Glu-269 to the terminal Ser residue using forward primer 5′-TAGAATTCGAGGACTGGCACAGCCG-GAGGAA-3′ and reverse primer 5′-TACTCGAGTCATGAA-CATAACCCGCGGCTGTG-3′. Fragments were subcloned into EcoRI/XhoI sites of pGEX4T-1, and proteins were expressed in *E. coli* according to manufacturer instructions and purified with glutathione agarose (Amersham Biosciences). Human Hck, Lyn, and c-Src were expressed in Sf9 insect cells and purified to homogeneity as previously described (10). The C-terminal sequence of each SFK was modified to Tyr-Glu-Glu-Ile-Pro, which promotes autophosphorylation of the tail tyrosine and permits high yield purification of the downregulated form of each kinase (10). The SF2 allele of HIV-1 Nef was expressed in bacteria and purified as previously described (10).

Phage Display. The phage-displayed SH3 domain library panning onto purified target proteins was performed as previously described (11). Briefly, six-well tissue culture plates (Cellstar) were coated with 20 μg/ml bacterially expressed purified GST fusion proteins of the GPVI C-tail and the GPVI C-tail lacking the PD sequence or, in control experiments, GST protein alone (1.5 ml per well) in 50 mM Na-carbonate buffer pH 9.6 overnight at 4 °C. The subsequent steps were performed at room temperature. The plates were washed three times with 2 ml of TBS-T buffer [Tris-buffered saline (TBS) supplemented with 0.05% Tween 20] and incubated with blocking solution (5% nonfat milk in TBS-T) for 2h, followed by incubation with the mixture of human SH3 library-displaying phages (109–1,010 pfu/well) prepared in TBS-T and supplemented with 2.5% of nonfat milk for 2 h. Subsequently, the phage mixture was removed and plates were washed four times with 2 ml of TBS-T. The infection of TG1 bacteria by phages that remained bound to GPVI C-tail proteins or GST alone was carried out by adding 1 ml of log-phased cells (OD_{600} = 0.5–0.6) to each well followed by incubation at 37 °C for 1 h. Subsequently, different dilutions of infected TG1 (1:1, 1:10, 1:100, and 1:1,000) were seeded onto ampicillin-containing LB plates. The next day, the resultant colony numbers from WT GPVI C-tail and from PD GPVI C-tail were compared to the number of colonies obtained from the control (GST alone) plate. WT GPVI C-tail-interacting SH3 domains were identified by performing a sequencing reaction (sequencing primer 5′-CCTATTGCCTACGGCAGCC-3′) on the SH3 domain-encoding phagemides that were isolated from individual bacterial colonies.

Immunoprecipitations from Platelet or RBL-2H3 Cell Lysate. Blood was collected from five healthy donors into 30- or 60-ml syringes containing 5 or 10 ml of acid citrate dextrose. Platelets were isolated from PRP by centrifugation in the presence of 1 U/ml apyrase and 1 μM prostacyclin and washed once in platelet wash buffer (10 mM Hepes, 1 mM EDTA, 150 mM NaCl, pH 6.0)

before resuspending in modified Tyrode's buffer. Washed platelets (6×10^8) were stimulated with 10-nM convulxin or left unstimulated at 37 °C with stirring, and reactions were terminated with addition of 5× lysis buffer (1% Nonidet P-40, 50 mM Tris pH 7.4, 150 mM NaCl, 2 mM EDTA final concentration) with a 1:50 dilution of EDTA-free protease inhibitor mixture (Roche Diagnostics) and a 1:100 dilution of HaltTM phosphatase inhibitor mixture (Thermo Scientific). Transfected RBL-2H3 cells were incubated in RPMI at 37 °C for 30 min at a concentration of 1×10^7 cells/ml. Next, 6×10^6 RBL-2H3 cells were stimulated with 1-nM convulxin or left unstimulated at 37 °C with stirring, and reactions were terminated with addition of an equal volume of ice-cold 2× Nonidet P-40/dodecyl maltoside lysis buffer (1.6% Nonidet P-40, 2% dodecyl maltoside, 20 mM Tris, pH 7.5, 300 mM NaCl, 4 mM EDTA, 2 mM DTT) (12), with protease and phosphatase inhibitors as described above. Samples were lysed for 1 h at 4 °C, and insoluble material was pelleted by centrifugation at $15{,}000 \times g$ for 20 min. For GST-fusion immunoprecipitation, lysate was incubated with glutathione-Sepharose beads conjugated with GPVI GST-fusion protein. For GPVI immunoprecipitation, lysate was incubated with 5 μg/ml HY101 monoclonal antibody or 5 μg/ml mouse IgG for 2 h at 4 °C before addition of protein-A Sepharose and overnight incubation with rocking. Sepharose beads were pelleted and washed four times for 5 min in 1× lysis buffer before addition of Laemmli sample buffer with 2.5% β-mercaptoethanol and boiling for 10 min. Samples were run on 4 to 12% vol/vol gradient SDS-polyacrylamide using Mops electrophoresis buffer, transferred to PVDF membranes, blocked, and probed with antibody.

In Vitro Kinase Assays. Production of recombinant HIV-1 Nef and tyrosine kinase assays were performed in 384-well plates using the Z'Lyte kinase assay system and the Tyr-2 peptide substrate (Invitrogen) (10). To assess the effect of GPVI compared to Nef on SFK activity, Hck (20 ng), Lyn (50 ng), or c-Src (50 ng) was incubated at room temperature for 5 min with increasing molar concentrations of GST-WT GPVI, GST–PD GPVI, or Nef. Purified GST-fusion proteins were dialyzed to remove free glutathione before use in in vitro kinase assays. ATP (100 μM final) and Tyr-2 substrate (1 μM final) were then added to the reaction, and samples were incubated for 1 h (45 min for Hck). Development reagent, which contains a protease that digests nonphosphorylated peptide, was then added, and samples were incubated for an additional 60 min before termination of the reaction with stop reagent. Fluorescence was assayed, based on FRET between coumarin and fluorescein in the phosphorylated (uncleaved) substrate peptide only. Raw fluorescence values were corrected for background, based on a 0% phosphorylation (no ATP) negative control, and reaction endpoints were calculated as emission ratios of coumarin fluorescence divided by the fluorescein FRET signal. These ratios were then normalized to the ratio obtained with a 100% phosphorylation control peptide. Each condition was assayed in quadruplicate, and results are presented as the mean ± SD.

Statistics. *P* values were calculated using an unpaired two-tailed Student's *t*-test assuming unequal variance.

1. Chan VW, Meng F, Soriano P, DeFranco AL, Lowell CA (1997) Characterization of the B lymphocyte populations in Lyn-deficient mice and the role of Lyn in signal initiation and down-regulation. *Immunity* 7:69–81.
2. Kato K, et al. (2003) The contribution of glycoprotein VI to stable platelet adhesion and thrombus formation illustrated by targeted gene deletion. *Blood* 102:1701–1707.
3. Chen H, Locke D, Liu Y, Liu C, Kahn ML (2002) The platelet receptor GPVI mediates both adhesion and signaling responses to collagen in a receptor density-dependent fashion. *J Biol Chem* 277:3011–3019.
4. Sebzda E, et al. (2006) Syk and Slp-76 mutant mice reveal a cell-autonomous hematopoietic cell contribution to vascular development. *Dev Cell* 11:349–361.
5. Suzuki-Inoue K, et al. (2002) Association of Fyn and Lyn with the proline-rich domain of glycoprotein VI regulates intracellular signaling. *J Biol Chem* 277:21561–21566.
6. Zou Z, Chen H, Schmaier AA, Hynes RO, Kahn ML (2007) Structure-function analysis reveals discrete beta3 integrin inside-out and outside-in signaling pathways in platelets. *Blood* 109:3284–3290.
7. Pear WS, et al. (1998) Efficient and rapid induction of a chronic myelogenous leukemia-like myeloproliferative disease in mice receiving P210 bcr/abl-transduced bone marrow. *Blood* 92:3780–3792.
8. Ohmori T, et al. (2007) Silencing of a targeted protein in in vivo platelets using a lentiviral vector delivering short hairpin RNA sequence. *Arterioscler Thromb Vasc Biol* 27:2266–2272.
9. Neeves KB, et al. (2008) Microfluidic focal thrombosis model for measuring murine platelet deposition and stability: PAR4 signaling enhances shear-resistance of platelet aggregates. *J Thromb Haemost* 6:2193–2201.
10. Trible RP, Emert-Sedlak L, Smithgall TE (2006) HIV-1 Nef selectively activates Src family kinases Hck, Lyn, and c-Src through direct SH3 domain interaction. *J Biol Chem* 281:27029–27038.
11. Karkkainen S, et al. (2006) Identification of preferred protein interactions by phage-display of the human Src homology-3 proteome. *EMBO Rep* 7:186–191.
12. Tomlinson MG, et al. (2007) Collagen promotes sustained glycoprotein VI signaling in platelets and cell lines. *J Thromb Haemost* 5:2274–2283.

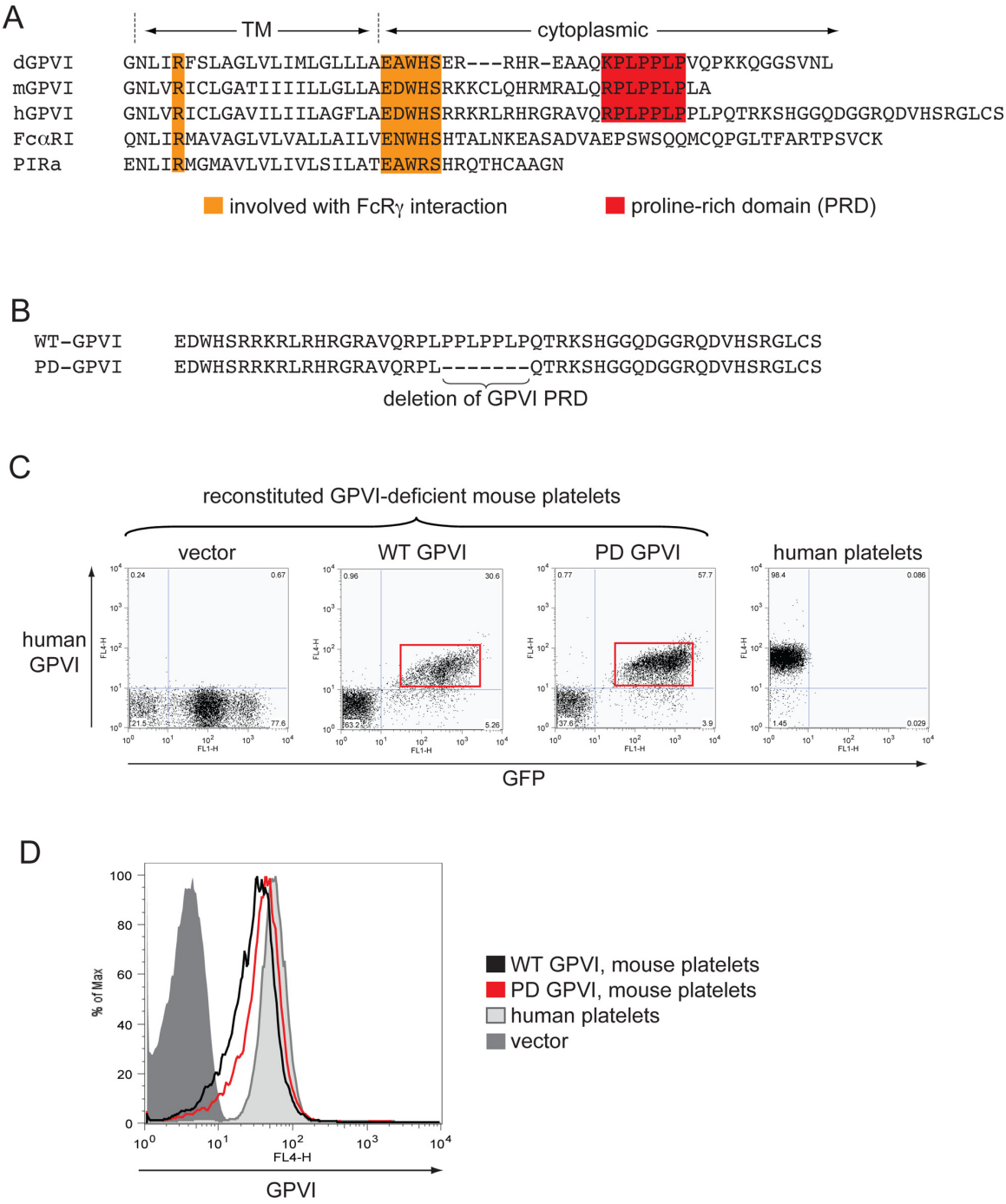

Fig. S1. Expression of wild-type GPVI receptors and GPVI receptors lacking the intracellular PRD in GPVI-deficient mouse platelets using retroviral vectors. (*A*) Alignment of the predicted transmembrane and intracellular amino acid sequences from opossum (d), mouse (m), and human (h) genes encoding the GPVI receptor, the homologous and paralogous human Fc alpha receptor (FcαRI), and the mouse paired Ig-like receptor (PIR)a. The amino acids shown in orange are involved in coupling of the receptor to the transmembrane signaling adaptor FcRγ. The amino acids shown in red constitute a binding motif for SH3 domains. Note the lack of the GPVI PRD in homologous immune receptors. (*B*) The amino acid sequences of the cytoplasmic tails of the wild-type human GPVI (WT GPVI) and mutant GPVI lacking the proline-rich region of the cytoplasmic tail (PD GPVI) are shown. The sequence of the cytoplasmic tail of human PD GPVI lacked 7-aa residues unique to the PRD and was identical to that shown by Suzuki-Inoue et al. to no longer bind SFK SH3 domains [Suzuki-Inoue K, et al. (2002) Association of Fyn and Lyn with the proline-rich domain of glycoprotein VI regulates intracellular signaling. *J Biol Chem* 277(24):21561–21566.]. (*C*) Retroviral coexpression of GPVI receptors and GFP in GPVI-deficient mouse platelets. Retroviral vectors were used to coexpress GFP only (vector), or GFP with either WT GPVI or PD GPVI, in GPVI-deficient fetal liver cells that were subsequently used to reconstitute lethally irradiated mice. Shown are GFP and surface GPVI expression in the platelets of animals reconstituted with cells exposed to empty vector (vector), vector driving expression of WT GPVI, vector driving expression of PD GPVI, and human platelets. GFP+ platelets expressing surface WT GPVI and PD GPVI are shown in red boxes. (*D*) Expression levels of human GPVI on mouse platelets. Shown are histograms of surface GPVI in GFP-positive platelets from the indicated reconstituted mice compared to GPVI on human platelets.

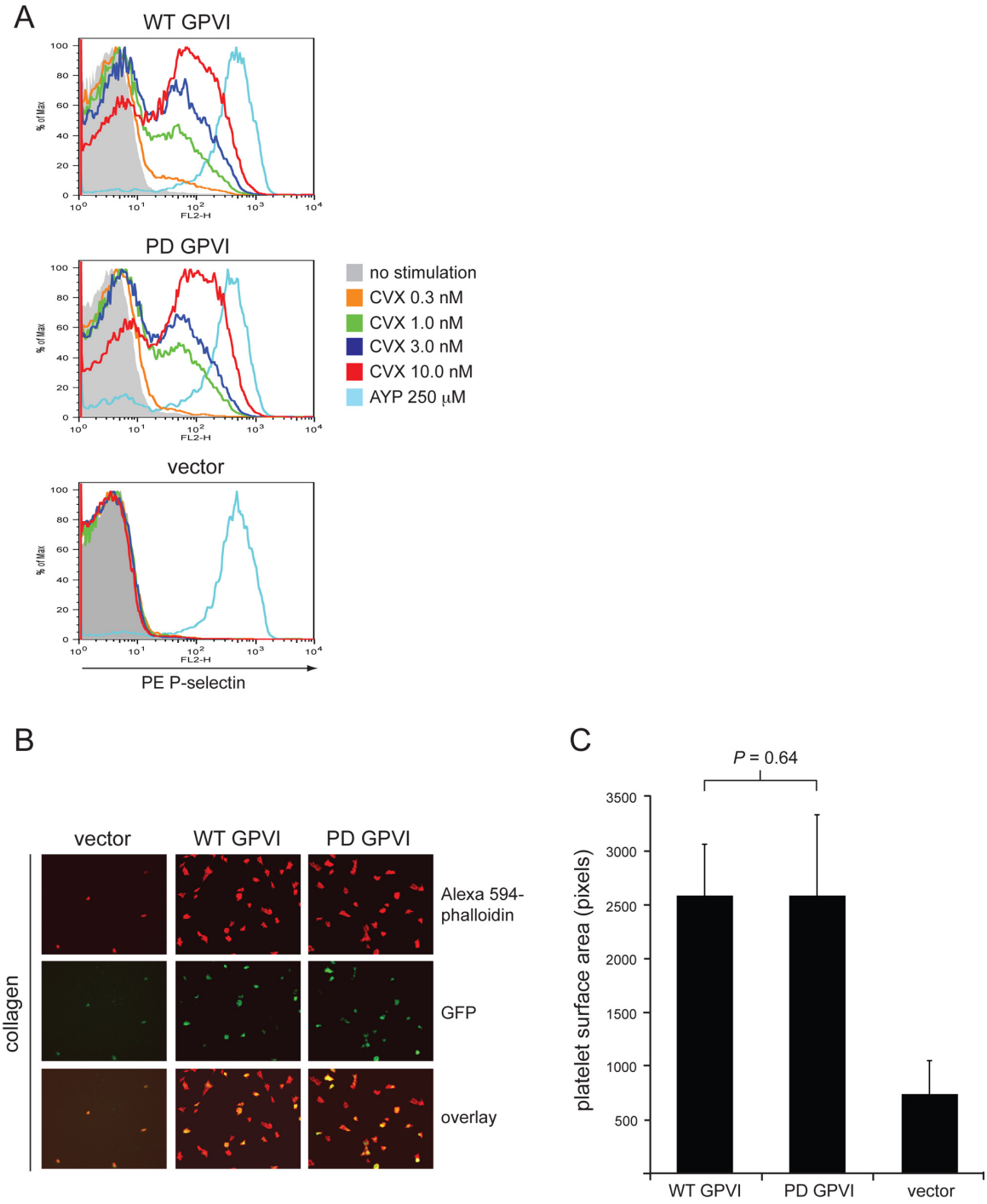

Fig. S2. Loss of the GPVI PRD does not alter sustained GPVI receptor signaling in platelets. (*A*) Platelet activation mediated by WT and PD GPVI signaling. Platelets from GPVI-deficient mice expressing WT GPVI or PD GPVI receptors were stimulated with the indicated concentrations of convulxin for 10 min, and activation was measured using flow cytometry to detect the expression of surface P-selectin in GFP+, GPVI-expressing platelets. AYP indicates exposure to the PAR4 agonist peptide AYPGKF. (*B*) Platelet spreading on collagen mediated by WT or PD GPVI. Platelets from the indicated mice were incubated for 45 min on immobilized type-I collagen, and spreading was visualized by staining with Alexa-Fluor 594-conjugated phalloidin to detect cellular actin. GFP expression was simultaneously measured to identify platelets derived from vector-transduced precursors. (*C*) Quantitation of platelet spreading driven by WT GPVI or PD GPVI, depicted in (*B*). The area occupied by adherent platelets was measured using the Image J program. n = 100 to 300 individual platelets from two to three different animals analyzed for WT or PD GPVI or vector control.

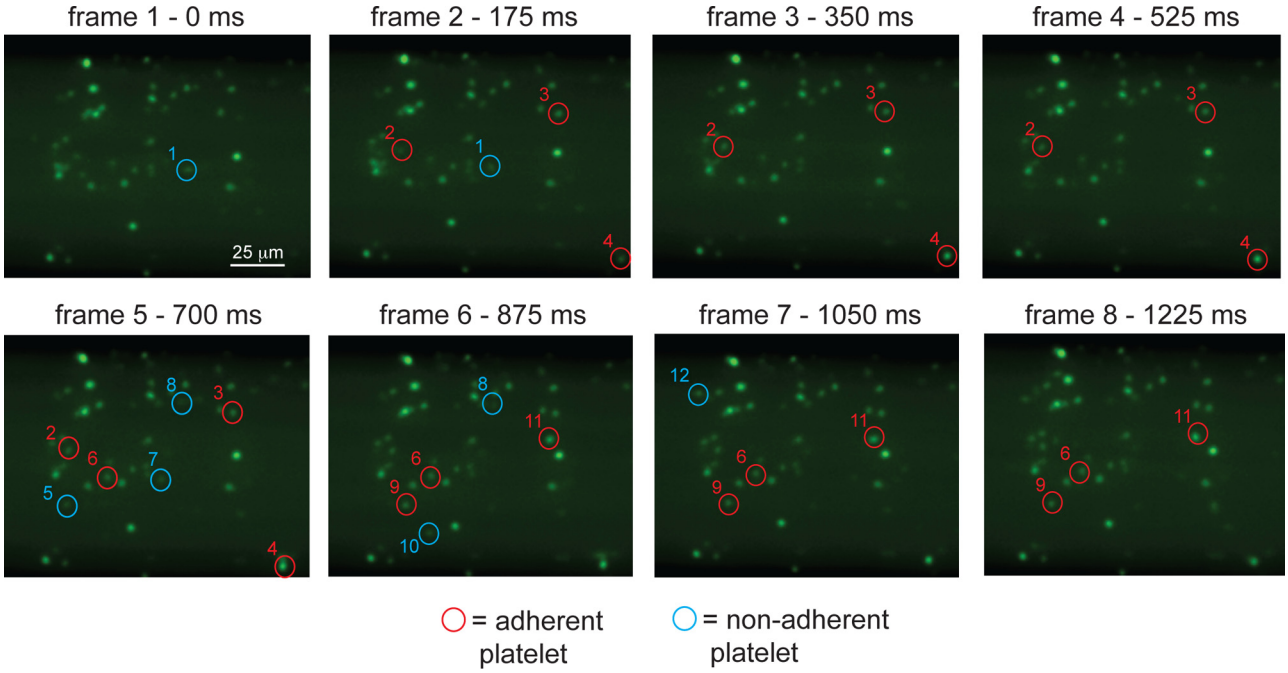

Fig. S3. Tracking rolling and adhesion of GFP+/GPVI+ platelets to collagen under flow. Measurement of platelet adhesion efficiency during flow over a collagen-coated surface. Shown is an example of sequential images taken with a 75-ms exposure time during flow of whole blood containing WT GPVI-expressing platelets over a type-I collagen-coated surface. Blood from reconstituted mice was flowed over a patterned type-I collagen strip at a shear rate of 1,000 s^{-1}, and fluorescent images were taken every 100 ms to follow the interaction of GFP+ platelets with collagen under flow. Each platelet that appears on the collagen strip was tracked to determine if it remained adherent (red circles) or did not remain adherent (blue circles). Adhesive efficiency was determined by $a/(a + r)$, where a = the number of platelets that permanently adhere and r = the number of platelets that roll along collagen but do not adhere. The direction of flow and translocation of platelets is from left to right.

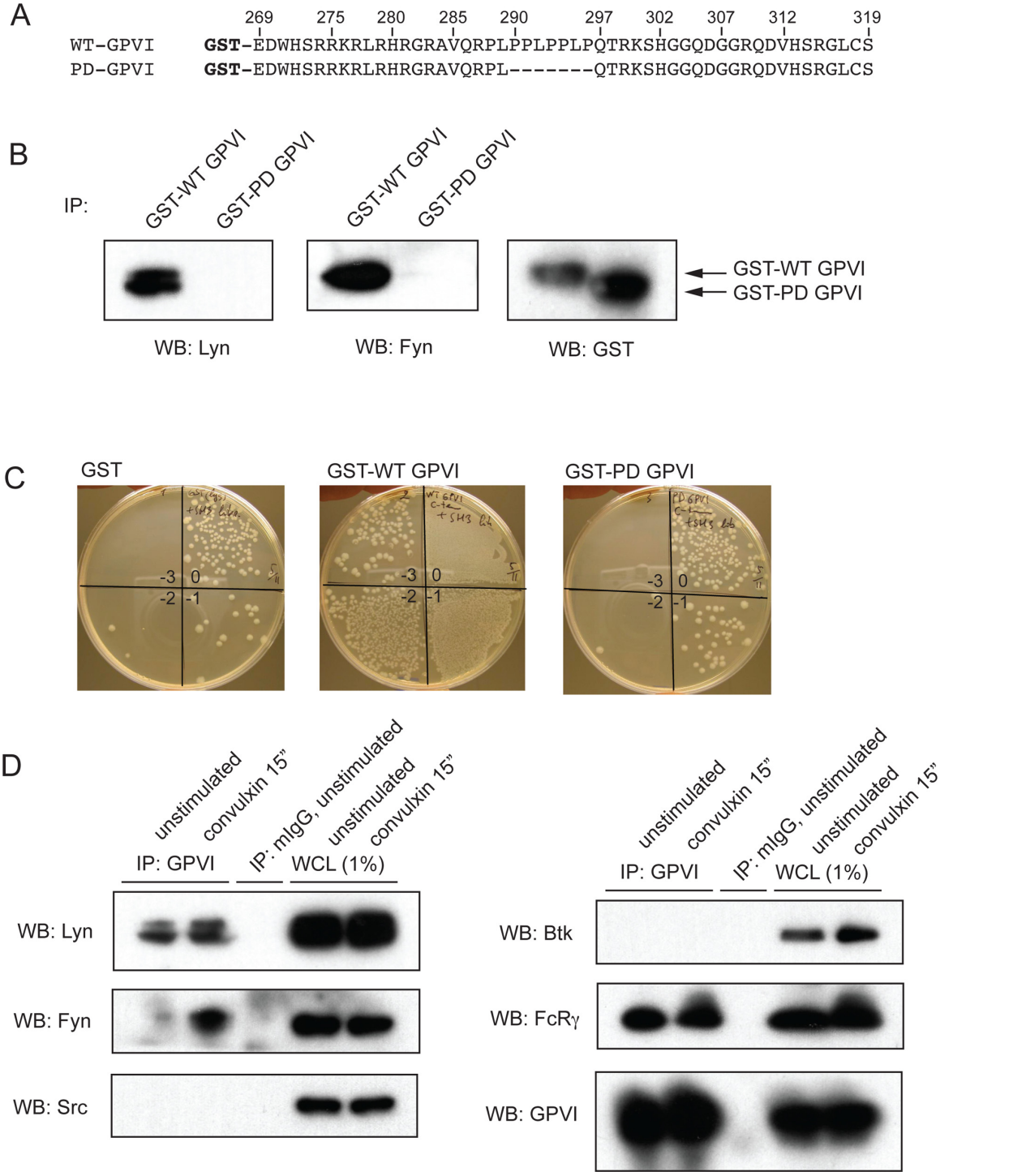

Fig. S4. The GPVI PRD preferentially binds the SH3 domains of the SFKs Lyn and Hck. (*A*) Shown are the amino acid sequences of the cytoplasmic tail of WT GPVI and PD GPVI expressed as GST-fusion proteins. (*B*) Binding of SH3 domain-containing proteins from platelet lysate is dependent on the GPVI PRD. Washed human platelets were lysed, and platelet proteins were precipitated with either GST-WT GPVI or GST-PD GPVI bound to glutathione beads, resolved by SDS/PAGE, and analyzed by immunoblotting (WB) for Lyn, Fyn, or GST. (*C*) Phage display screening of WT or PD GPVI GST-fusion protein binding to human SH3 domains, an unbiased method in which all SH3 domains compete with each other for binding to the target protein. SH3 domain-expressing phages captured by GST-GPVI constructs or plain GST were used to infect *E. coli* TG1 cells and plated as 10-fold dilutions onto ampicillin plates. Enrichment of SH3 displaying phages bound to the WT GPVI receptor was ≈1,000-fold compared to that bound to PD GPVI or GST alone. (*D*) Lyn constitutively associates with GPVI in unstimulated platelets. Washed human platelets were left unstimulated or stimulated with 3 nM convulxin for 15 s, lysed, and proteins immunoprecipitated (IP) with GPVI were resolved by SDS/PAGE and analyzed by immunoblotted (WB) for Lyn, Fyn, Src, Btk, FcRγ, or GPVI. An immunoblot of whole-cell lysate (WCL), loaded at 1% of GPVI IP input, and one of mouse IgG control IP are also shown. Blots depicted are representative of three independent experiments.

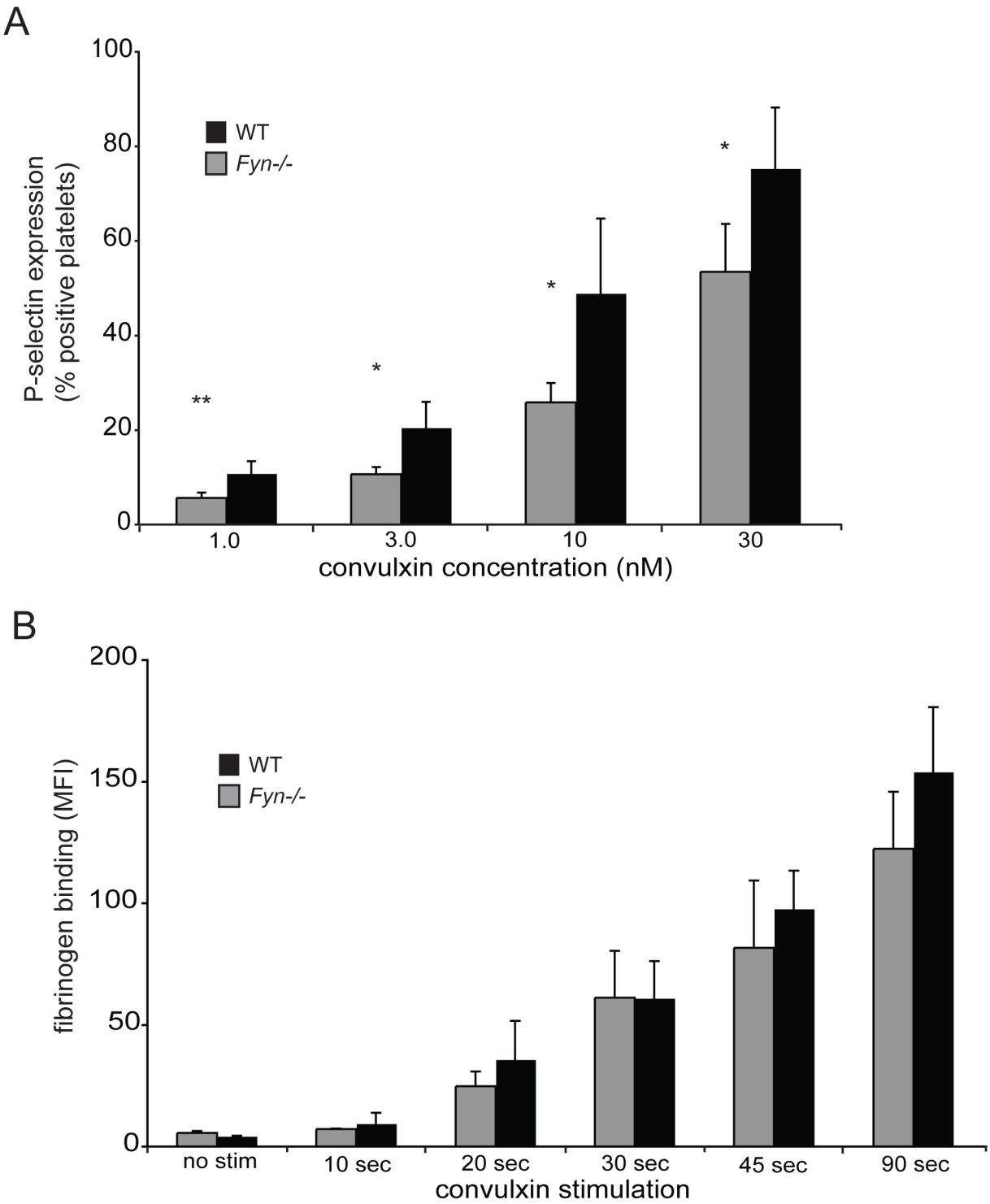

Fig. S5. Fyn-deficient platelet activation following convulxin stimulation. (*A*) Platelets from *fyn*$^{-/\text{minus}]}$ mice or wild-type littermate controls (WT) were stimulated with the indicated concentrations of convulxin for 10 min, and P-selectin expression was determined by flow ctyometry. Bars indicate % P-selectin positive platelets. (*B*) Time-course of platelet fibrinogen binding following convulxin stimulation. Platelets were stimulated with 10-nM convulxin in the presence of Alexa-Fluor 647-conjugated fibrinogen for times indicated, fixed, and analyzed by flow cytometry. Bars indicate mean fluorescent intensity (MFI) of fibrinogen binding. For (*A*) and (*B*), *P*-values were calculated; *, $P < 0.05$; **, $P < 0.01$; error bars indicate mean ± SD; n = four to six experiments using three mice of each genotype for each concentration of convulxin or time point.

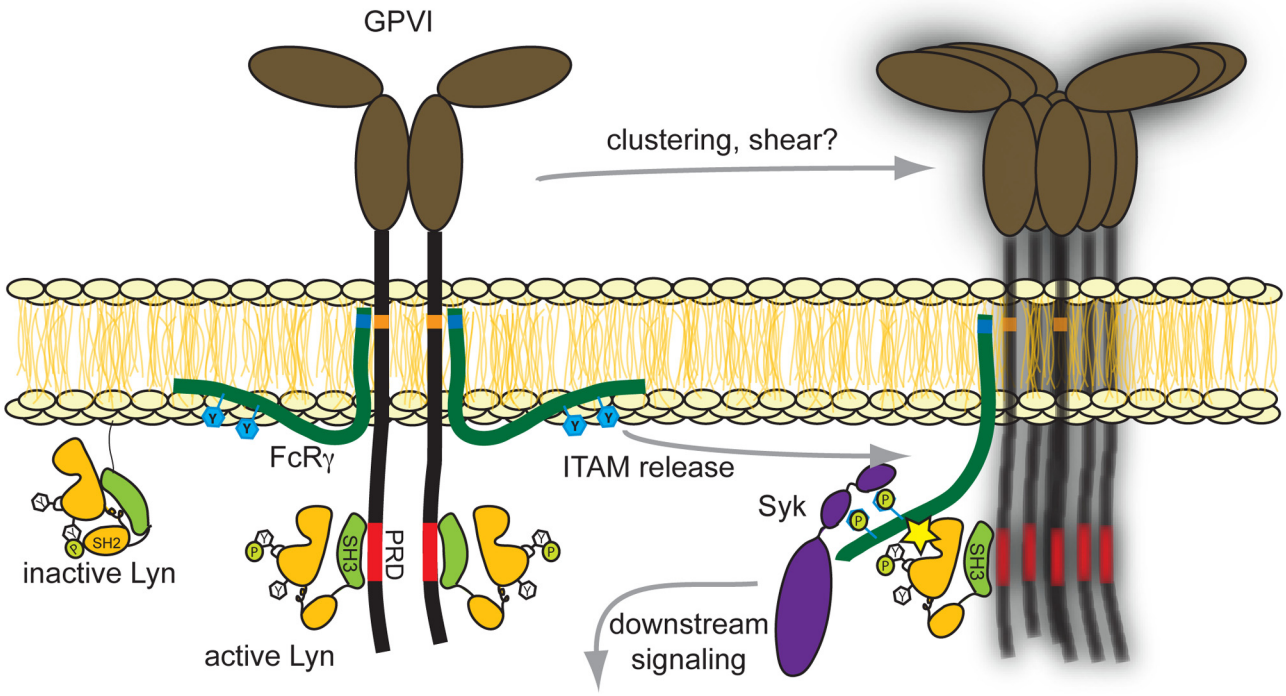

Fig. S6. Priming of Lyn by the GPVI PRD drives rapid signal transduction following receptor ligation. In this model, Lyn is held in an activated state when constitutively bound to GPVI through displacement of the Lyn SH3 domain (*light green*) by the GPVI PRD (*light red*). Premature, ligand-independent receptor signaling is prevented by sequestration of the GPVI-associated FcRγ chain (*dark green*) within the lipid bi-layer, keeping ITAM domains (*light blue*) inaccessible to activated Lyn before receptor ligation [Xu C, et al. (2008) Regulation of T cell receptor activation by dynamic membrane binding of the CD3epsilon cytoplasmic tyrosine-based motif. *Cell* 135(4):702–713.] . Following GPVI-collagen binding, the FcRγ chain is released from the membrane by clustering or mechanical shear forces, allowing GPVI-bound, activated Lyn to phosphorylate the FcRγ ITAM. ITAM phosphorylation results in recruitment of Syk (*purple*) and initiation of the downstream GPVI signaling cascade.

Table S1. The GPVI cytoplasmic tail preferentially binds the SFKs Lyn and Hck

	Number of clones			
SH3 domain	Screen #1	Screen #2	Screen #3	Total
Lyn	4/8clones	10/24clones	2/16clones	16/48clones
Hck	1/8clones	10/24clones	8/16clones	19/48clones
Fyn	1/8clones	1/24clones	0/16clones	2/48clones
Btk	1/8clones	1/24clones	2/16clones	4/48clones
Yes	1/8clones	0/24clones	2/16clones	3/48clones
Src	0/8clones	0/24clones	0/16clones	0/0clones
CrkL	0/8clones	1/24clones	0/16clones	1/48clones
Intersectin 1 third SH3 domain	0/8clones	1/24clones	2/16clones	3/48clones

The identity of the SH3 domains bound by GST-WT GPVI proteins was determined by sequencing the inserts of the selected phage clones after a single round of affinity selection. Shown are sequencing results of bacterial clones containing the phagemide encoding the corresponding SH3 domain bound to WT GPVI. Results demonstrate GPVI intracellular tail binding preference for SFKs, specifically Lyn and Hck.